Polarimetric Investigation of a Two Surface Layer Structure

Noora Al-Kahachi, Konstantinos Panagiotis Papathanassiou.
Deutsches Zentrum für Luft- und Raumfahrt (DLR), Oberpfaffenhofen, Germany

Abstract

One of the challenges of future planetary SAR missions will be the estimation of surface and subsurface geometric and dielectric characteristics. In this sense an analytical model of a two layer structure, with small scale roughness, is proposed optimized for lower frequencies. The model takes into account the distributed nature of surface and subsurface. The recovery of the sub-surface physical properties is discussed by means of 2 incident angles. Simulation results and noise robustness of the inversion model are shown.

1 Introduction

The knowledge of the rocks' type or the determination of moisture content of buried structures using SAR, can reveal geological facts. Both tasks can be solved through the knowledge of the subsurface permittivity. The considered structure consists of two layers as it is shown in Fig. 1.

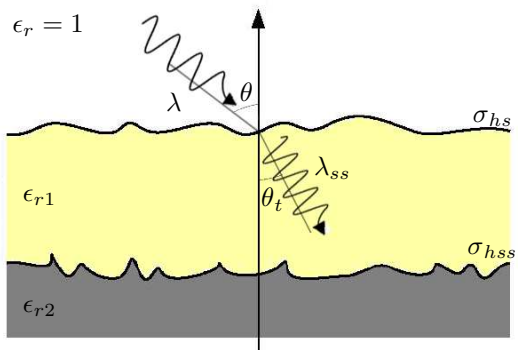

Figure 1: Two layer scattering model

The scattering process at a two layer structure for the monostatic case excluding the multiply reflection, can be expressed by

$$[S_t] = [P_1]([S_s] + [\Gamma][P_2][S_{ss}][P_2]^T[\Gamma]^T)[P_1]^T + [N]. \quad (1)$$

The electromagnetic wave propagates through space, undergoes atmospheric ans Ionospheric disturbance summarized in $[P_1]$. A part of it is scattered on the upper surface, described by the scattering matrix $[S_s]$ that depends on the surface properties including permittivity and roughness. Another part penetrates into the layer (transmission coefficients $[\Gamma]$) with a smaller wavelength (λ_{ss}) and incident angle (θ_t), as indicated in Figure 1. The propagation of the transmitted electromagnetic field through the medium is described by $[P_2]$. The subsurface scatters back to the radar ($[S_{ss}]$), where it propagates again through the layer and the atmosphere. The matrix $[N]$ stands for the additive noise contribution.

The backscattering at the surface is modeled by the Small Perturbation Method (SPM), also known as Bragg [1]. SPM introduces backscattering that depends on several parameters including roughness (σ_{hs}), wavelength (λ) and the incident angle (θ). The subsurface is also modeled using the SPM, but assuming a different roughness (σ_{hss}). The incident angle and the wavelength are changed because of the boundary conditions and the different electromagnetic speed through the medium. Since the surface and the subsurface interfaces are distributed and uncorrelated, then the backscattering from the interfaces can not be added coherently.

In terms of the polarimetric coherency matrix for surface and subsurface. The incoherent addition of their backscattering contribution is a straight forward addition of the coherency matrices. The sum corresponds to the total system coherency matrix

$$[T_t] = [P_3^1]([T_s] + [P_3^2][T_{ss}][P_3^2]^T)[P_3^1]^T + [N]. \quad (2)$$

The propagation matrices are assumed to be polarimetric independent and are modeled as weighted 3 by 3 unitary matrices. A better interpretation of the system scattering behavior is obtained by considering the polarimetric coherency matrix and can achieve good modeling of the roughness polarimetric effects in future work.

2 Two layer polarimetric scattering model

Two parallel Bragg layers are considered. The radar cross section RCS dependency on λ and θ for a single Bragg

surface is shown in equation (3), as presented by [1]

$$\sigma_{S,P} = 8k^4\sigma_h^2 \cos^4\theta \cdot |R_{S,P}|^2 \cdot W(2k\sin\theta, 0). \quad (3)$$

The influence of the incident angle and the wavelength on the RCS and the polarimetric coherency matrix power (the T matrix pre-factor) is similar, as shown in equation (4). The polarimetric coherency matrix of the surface is of a rank one matrix and given by

$$[T_s] = m\sigma_{hs}^2 \left(\frac{\cos\theta}{\lambda}\right)^4 f_s \begin{bmatrix} 1 & B_s^* & 0 \\ B_s & |B_s|^2 & 0 \\ 0 & 0 & 0 \end{bmatrix}. \quad (4)$$

The equation is derived from references [1] and [5]. Here m is a system related factor. The suffix s indicates the surface. f_s is proportional to the surface backscattering power, B_s has a value range between 0 and -1, and they are given by

$$\begin{aligned} f_s &= \frac{|R_{Ss} + R_{Ps}|^2}{2} \\ B_s &= \frac{R_{Ss} - R_{Ps}}{R_{Ss} + R_{Ps}}. \end{aligned} \quad (5)$$

For the subsurface, the transmission and attenuation effects are considered. The coherency matrix is also of a rank one and given by

$$[T_{ss}] = m\sigma_{hss}^2 \left(\frac{\cos\theta_t}{\lambda_{ss}}\right)^4 f_{ss}A^2 \begin{bmatrix} 1 & B_{ss}^* & 0 \\ B_{ss} & |B_{ss}|^2 & 0 \\ 0 & 0 & 0 \end{bmatrix}. \quad (6)$$

The suffix ss indicate the subsurface. f_{ss} and B_{ss} are given by

$$\begin{aligned} f_{ss} &= \frac{|\Gamma_\perp R_{Sss} + \Gamma_\parallel R_{Pss}|^2}{2} \\ B_{ss} &= \frac{\Gamma_\perp R_{Sss} - \Gamma_\parallel R_{Pss}}{\Gamma_\perp R_{Sss} + \Gamma_\parallel R_{Pss}}. \end{aligned} \quad (7)$$

According to Equation (3), the roughness σ_h affects only the powers that correspond to the interface, but not the power ratios for different polarisations. This is a characteristic of SPM.

As explained before, since the surface and subsurface are uncorrelated, then the addition of their coherency matrices corresponds to the received coherency matrix for the total system $[T_t]$, as given by

$$\begin{aligned} [T_t] = m\sigma_{hs}^2 \left(\frac{\cos\theta}{\lambda}\right)^4 f_s \begin{bmatrix} 1 & B_s^* & 0 \\ B_s & |B_s|^2 & 0 \\ 0 & 0 & 0 \end{bmatrix} + \\ m\sigma_{hss}^2 \left(\frac{\cos\theta_t}{\lambda_{ss}}\right)^4 f_{ss}A^2 \begin{bmatrix} 1 & B_{ss}^* & 0 \\ B_{ss} & |B_{ss}|^2 & 0 \\ 0 & 0 & 0 \end{bmatrix}. \end{aligned} \quad (8)$$

Since in general $T_{11} \cdot T_{22} \neq T_{12} \cdot T_{21}$ (equal only when $B_s^* = B_{ss}^*$) the total coherency matrix is a rank two matrix. This is different than for the single Bragg surface. The value for the second eigenvalue is very small and almost negligible. However its influence becomes important when the roughness effect increases and is considered by an upgraded model as the extended Bragg [5].

3 Model inversion

An inversion model for estimating the subsurface permittivity ϵ_{r2} is described in this section. Since achieving interferometry is difficult for planetary missions, the inversion of the polarimetric SAR data using angular diversity is discussed. In the inversion algorithm, the knowledge of data acquired from two different incident angles θ_1 and θ_2 is required. As a first step, the mean alpha angle α_t for both incident angles is calculated and a power ratio between the two incident angles $T_{11}(\theta_1)/T_{11}(\theta_2)$ is considered. From this information the subsurface to surface power ratio P_{ss}/P_s is estimated. In a second step, the subsurface and surface powers P_{ss}, P_s are estimated and used in the calculation of the subsurface coherency matrix $[T_{ss}]$. The combination of the subsurface alpha angles at two different incident angles $\alpha_{ss}(\theta_1)$ and $\alpha_{ss}(\theta_2)$ corresponds to a certain combination of surface and subsurface permittivity, which is obtained in the last step. A more detailed explanation is given in the following.

Step 1: Subsurface to surface power ratio estimation

The combination of two α_t from two incident angles for a single Bragg surface corresponds to a line for changing ϵ_{r1}, indicated by the red line in Figure 2. For the subsurface a line for each ϵ_{r2} value for different ϵ_{r1} is obtained, for example the blue line in Figure 2 given by ϵ_{r2}=8. ϵ_{r1} highly influences the subsurface polarimetric signature through the transmission coefficient as it has a certain difference between the horizontal and vertical polarisation.

The green area between the two lines in Figure 2 is the exact value of the two layer model α_t that is approximated by

$$\begin{aligned} \cos\alpha_t &= \frac{1}{\sqrt{1+|B_t|^2}} \quad , \\ |B_t|^2 &= \frac{P_s}{P_s+P_{ss}}|B_s|^2 + \frac{P_{ss}}{P_s+P_{ss}}|B_{ss}|^2. \end{aligned} \quad (9)$$

It approaches the subsurface line for higher subsurface to surface power ratio and the surface line for smaller ratio.

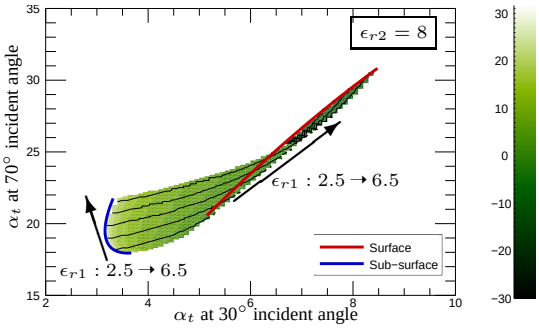

Figure 2: Subsurface to surface power ratio in dB for ϵ_{r2}= 8, 2.5$\leq \epsilon_{r1} \leq$6.5, at incident angles 70° and 30°.

Ambiguities in power ratio estimation arise because different blue lines in Figure 2 are obtained for different ϵ_{r2} values. For higher ϵ_{r2}, the curve lays in a higher alpha angle area.
The value of T_{11} at the higher incident angle divided by its value at a small incident angle $T_{11}(\theta_1)/T_{11}(\theta_2)$ is a power ratio that can be exploited to resolve this ambiguity. This ratio increases for higher ϵ_{r2}.

$$\frac{T_{11}(\theta_1)}{T_{11}(\theta_2)} = \frac{1 + P_{ss}(\theta_1)/P_s(\theta_1)}{1 + P_{ss}(\theta_2)/P_s(\theta_2)} \cdot \frac{P_s(\theta_1)}{P_s(\theta_2)}. \qquad (10)$$

Using these three values, a 3D look-up table is generated for estimating the power ratio at the large incident angle. A similar one is used for estimating the power ratio at the small incident angle.

Step 2: Subsurface alpha calculation

The obtained power ratio combined with T_t for both incident angles are used to obtain T_{ss} (see equation (8)). This is done by first calculating the subsurface and surface power dependency terms P_s, P_{ss}. Then, the other element of T_{ss} is calculated. From T_{ss}, the α_{ss} is obtained and used in further calculations. In the case of a very high subsurface to surface power ratio α_t can be considered directly equal to α_{ss}.

Step 3: Subsurface Permittivity estimation

The subsurface alpha like for the surface has a value range from 0° to 45°, but it is usually small. It shows the relation between the co-polarisation scattering coefficients. The difference between the subsurface co-polarisation scattering coefficients depends basically on the incident angle, ϵ_{r2} and ϵ_{r1} through the transmission coefficient and the reflection coefficient, through equation (7). α_{ss} increases with increasing incident angle and for larger values of ϵ_{r2}. The roughness also affects alpha, but not for the Bragg model.
For a known incident angle, α_{ss} is a function of ϵ_{r1} and ϵ_{r2} values. With a second incident angle, a unique solution for the permittivity values is obtained.

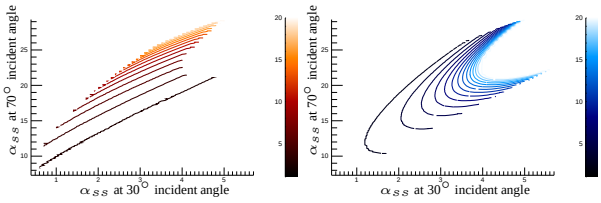

(a) Surface Permittivity. (b) Subsurface Permittivity.

Figure 3: ϵ_{r1} and ϵ_{r2} as functions of α_{ss} at 70° and 30° incident angles.

The estimation of ϵ_{r2} is not so sensitive to α_{ss} for small values of ϵ_{r1} as it is for higher values, since the contour lines in Figure 3(b) are closer to each other in the region of high ϵ_{r1} that are pointed out in Figure 3(a).

4 Simulation results

The described model is implemented, and the performance error and model noise robustness are investigated.

4.1 Extraction of subsurface parameters

The inversion model sensitivity is shown in the following part where the results are averaged over different upper layer attenuation values and a roughness ranges ($2\pi\sigma_h/\lambda$) from 0.1 to 0.3 for both surface and subsurface. It can be interpreted through the effect of quantization in the look-up tables on the inversion of noiseless data. A better estimation for ϵ_{r2} is achieved when ϵ_{r1} is smaller (see Figure 4). An estimation of ϵ_{r2} under a rocky surface ($\epsilon_{r1} \geq 4.5$) is so inaccurate since an error of 0.1° in the α_{ss} induce an estimation error of 10% for incident angles 70° & 30°.

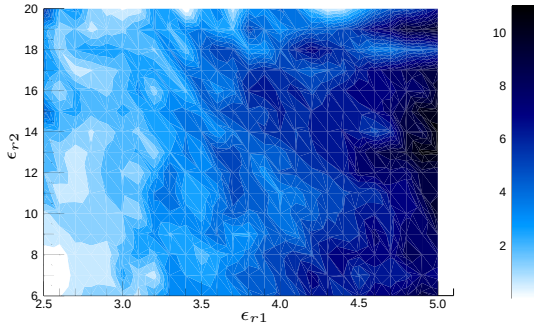

Figure 4: Estimation error (in %) of ϵ_{r2} at 30° and 70°

To evaluate a best combination of incident angles, an investigation of the error percentage for different angle combinations is performed. The average value of the error percentage for a certain angle combination is obtained from averaging over the error in the range of 3$\leq \epsilon_{r1} \leq$4.5 and 8$\leq \epsilon_{r2} \leq$14.

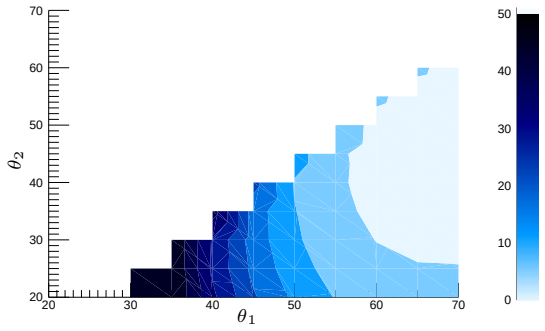

Figure 5: Estimation error (in %) of ϵ_{r2} for different combination of θ with a 5° resolution

The results shows that the error is smaller for higher incident angles, where the alpha range is larger and the polarimetric noise effect is smaller. It can also be noticed that a better estimation is achieved when the angles are enough separated (by more than 5°) and not so close to the diagonal in Figure 5.

4.2 Estimation of noise robustness

Noise is modelled as Gaussian white noise, which has no polarimetric structure. The white noise effect can be modelled by adding a unitary matrix that is waited by the noise power.

$$[T]_{\text{noisy}} = [T]_{\text{noiseless}} + N[I]. \tag{11}$$

The same noise power is added to all [T]-matrices of different incident angles. The signal to noise ratio used here is calculated relative to the signal power at 40° incident angle. The α_{ss} estimation is less accurate for lower values of ϵ_{r2} where α_{ss} is smaller.
The estimation of the ϵ_{r2} in general follows α_{ss} estimation, but it is better in case of smaller ϵ_{r1} values, see Figure 6.

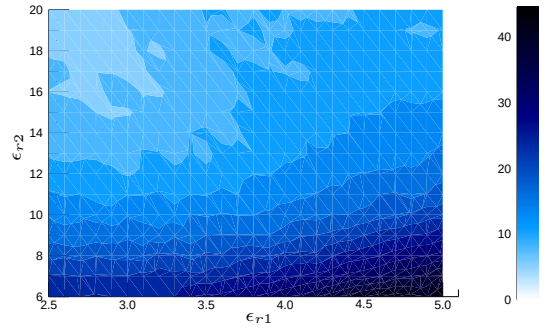

Figure 6: Estimation error (in %) of the ϵ_{r2}, for SNR = 30 dB.

For different angle combinations, the noise highly disturbs the estimation for small incident angles, therefore using higher angles offers a higher noise robustness and a separation of 10° seems enough, in spite of the low backscattered power.The Small Perturbation Method does not perform accurately at incident angles that are higher than 70° [1]. A range from 40° to 60° of incident angle with a 10° separation results in 30% error at 20 dB and 10% error at 30 dB in the estimation of ϵ_{r2}, according to this model, see Figure 7.

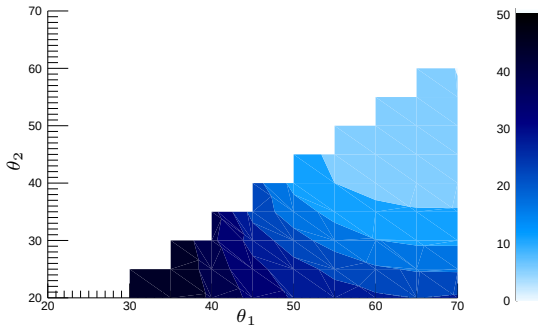

Figure 7: Estimation error (in %) of ϵ_{r2} for different combination of θ with a 5° resolution, for SNR = 30 dB.

5 Summary and next steps

For a two surface layer problem, a first investigation for extracting information about the subsurface permittivity, with a side looking SAR at low frequencies, has been discussed. Upper layer properties are required to be in a certain range, to allow enough backscattering from the subsurface, as for example relatively low permittivity and small roughness. A model for a slightly rough parallel surface and subsurface assuming a SPM backscattering from each interface is presented. Implementing the roughness effect on the polarimetric signature and resolving non parallel surface and subsurface interfaces are essential next steps. An inversion algorithm that requires observations with two different incident angles has been suggested here. Simulating the inversion model for the restricted two layer structure, shows the error in estimating the subsurface permittivity for a wide range of surface and subsurface roughness combinations.

References

[1] F. T. Ulaby: *Microwave Remote Sensing active and passive Vol.II*, (1982).

[2] H. Mott: *Remote sensing with polarimetric radar*, New York:Wiley, (2007).

[3] L. Tsang, J. Kong, and R. T. Shin: *Theory of Microwave Remote Sensing.*, New York: Wiley, (1985).

[4] A. Freeman and B. C. Campbell: *The 2-layer scattering problem*, IGARSS 2006.

[5] Irena Hajnsek: *Inversion of Surface Parameters using Polarimetric SAR*, Dissertation, DLR Oberpfaffenhofen, (2001).